PHYSICAL REVIEW D **88,** 025014 (2013)

Autocorrelation of density fluctuations for thermally relativistic fluids

Ryosuke Yano and Kojiro Suzuki

Department of Advanced Energy, University of Tokyo, 5-1-5 Kashiwanoha, Kashiwa, Chiba 277-8561, Japan

Hisayasu Kuroda

Department of Information Technology, University of Ehime, 3 Bunkyo-cho, Matsuyama, Ehime 790-8577, Japan

(Received 8 January 2013; revised manuscript received 6 March 2013; published 9 July 2013)

The autocorrelation of density fluctuations for thermally relativistic fluids is formulated on the basis of the relativistic Navier-Stokes-Fourier equation under the static equilibrium state. The autocorrelation of density fluctuations for thermally relativistic fluids, obtained theoretically, is compared with the autocorrelation of density fluctuations for thermally relativistic fluids, calculated using the stochastic relativistic Boltzmann equation on the basis of the direct simulation Monte Carlo method. The theoretical result of the autocorrelation of density fluctuations for thermally relativistic fluids on the basis of the relativistic Navier-Stokes-Fourier equation gives good agreement with the numerical result of the autocorrelation of density fluctuations for thermally relativistic fluids in the lowest wave number, because we calculated the autocorrelation of density fluctuations for thermally relativistic fluids under the transition regime between the rarefied and continuum regimes.

DOI: 10.1103/PhysRevD.88.025014 PACS numbers: 47.75.+f, 05.40.−a

I. INTRODUCTION

Recently, hydrodynamic fluctuations of the quark-gluon plasma (QGP) are focused [1], because the viscosity coefficient of the QGP obtained using experiments at RHIC [2] and LHC [3] might be explained by hydrodynamic fluctuations of the QGP on the basis of the fluctuation-dissipation theorem. In a recent paper by Kapusta *et al.* [1], the effect of hydrodynamic fluctuations on the Bjorken solution was investigated in detail. In this paper, we focus on the autocorrelation of density fluctuations for thermally relativistic fluids as an initial study of hydrodynamic fluctuations of the QGP. Here, thermally relativistic fluids are characterized using the thermally relativistic measure (χ) [4] by $0 < \chi = mc^2/(k\theta) \leq 100$ (m: mass of partons, c: speed of light, k: Boltzmann constant, θ: temperature), whereas we assume that m is large enough to realize $\chi \to 0$ by not $m \to 0$ but $\theta \to \infty$. Additionally, $\Lambda_{\mathrm{QCD}} \ll mc^2$ [5] is assumed. In particular, we categorize the thermally relativistic fluids with $\chi \leq 1$ as the thermally ultrarelativistic fluids [6]. Provided that $k\theta$ satisfies $\Lambda_{\mathrm{QCD}} \ll k\theta$, the asymptotic freedom of partons allows us to describe the QGP using the relativistic kinetic equation, which postulates the short range interaction among partons owing to the small running coupling constant [5,7]. Here, we use the stochastic relativistic Boltzmann equation to express a binary collision between two partons, whereas we must consider the three-body interaction to discuss the collision $gg \to ggg$ (g: gluon) [8]. In the energy regime of the asymptotic freedom, the collisional differential cross section depends on the momentum transferred between two colliding partons, and the collisional deflection angle also depends on the momentum, which is transferred between two colliding partons [5,7], whereas we assume that the thermally ultrarelativistic fluids are composed of hard spherical particles, which yield the constant collisional cross section and isotropic deflections of partons via binary collisions [9], to simplify our discussions. In this paper, we extend this assumption for thermally ultrarelativistic fluids to the thermally relativistic fluids, in which the assumption of the asymptotic freedom might be invalid. In the past study on the autocorrelation of density fluctuations for the relativistic fluids [10], thermally relativistic effects on density fluctuations were not discussed. In this paper, we consider the autocorrelation of density fluctuations for thermally relativistic fluids, which is affected by thermally relativistic effects, under the static equilibrium state in the laboratory frame. Therefore, the effect via the Lorentz contraction on density fluctuations is beyond the scope of this paper, and the Lorentz factor is fixed to unity. The autocorrelation of density fluctuations for thermally relativistic fluids is theoretically introduced and compared with the autocorrelation of density fluctuations for thermally relativistic fluids, which are obtained by solving the stochastic relativistic Boltzmann equation on the basis of the direct simulation Monte Carlo (DSMC) method [11].

II. FORMULATION OF AUTOCORRELATION OF DENSITY FLUCTUATIONS FOR THERMALLY RELATIVISTIC FLUIDS

The thermally relativistic Navier-Stokes-Fourier (NSF) equation with thermal fluctuations is obtained from Eqs. (A1), (A5), and (A6) in acausal form as follows [4],

$$\frac{\partial \rho}{\partial t} = -\boldsymbol{\nabla} \cdot (\rho \boldsymbol{v}), \tag{1}$$

$$\frac{\partial \rho v_i G}{\partial t} = -\frac{\partial}{\partial x_k}(p\delta_{ik} + \rho v_i v_k G - \Pi_{ik}), \quad (2)$$

$$\rho c_v \frac{\partial \theta}{\partial t} = -\rho c_v \boldsymbol{v}\cdot\nabla\theta - \nabla\cdot\boldsymbol{Q} - p\nabla\cdot\boldsymbol{v}, \quad (3)$$

where ρ is the density, $\boldsymbol{v} = (v_1, v_2, v_3)$ is the flow velocity, p is the static pressure, and $G \equiv K_3(\chi)/K_2(\chi)$, in which K_n is the nth order modified Bessel function of the second kind, Π_{ij} is the deviatoric stress tensor, $\boldsymbol{Q} = (Q_1, Q_2, Q_3)$ is the heat flux vector, and c_v is the specific heat at the constant volume. The formal difference between the thermally relativistic NSF equation and nonrelativistic NSF equation is a term G in Eq. (2). Consequently, the form of the thermally relativistic NSF equation coincides with the form of the nonrelativistic NSF equation, when $G = 1$, whereas c_v is a function of χ in the thermally relativistic fluids [9]. Under the static equilibrium state, Π_{ij} and $\boldsymbol{Q}$ are written as follows [1,12],

$$\Pi_{ij} = \eta\left(\frac{\partial v_i}{\partial x_j} + \frac{\partial v_j}{\partial x_i}\right) + \left(\zeta - \frac{2}{3}\eta\right)\delta_{ij}\frac{\partial v_l}{\partial x_l} + \delta\Pi_{ij}, \quad (4)$$

$$\boldsymbol{Q} = -\lambda\nabla\theta + \delta\boldsymbol{Q}, \quad (5)$$

where η is the viscosity coefficient, ζ is the bulk viscosity, and λ is the thermal conductivity, calculated for the hard spherical particles by Cercignani and Kremer [9] on the basis of Israel-Stewart theory.

In Eqs. (4) and (5), $\delta\Pi_{ij}$ is the deviatoric stress tensor generated by thermal fluctuations and $\delta\boldsymbol{Q}$ is the heat flux generated by thermal fluctuations. $\delta\Pi_{ij}$ and $\delta\boldsymbol{Q}$ yield the following relations [12]:

$$\begin{aligned}\langle \delta\Pi_{ij}(t,\boldsymbol{x})\cdot\delta\Pi_{kl}(t',\boldsymbol{x}')\rangle &= 2k\theta\left[\eta(\delta_{ik}\delta_{jl} + \delta_{il}\delta_{jk}) + \left(\zeta - \frac{2}{3}\eta\right)\delta_{ij}\delta_{kl}\right] \\ &\quad\times \delta(\boldsymbol{x}-\boldsymbol{x}')\delta(t-t'), \end{aligned}\quad (6)$$

$$\langle \delta Q_i(t,\boldsymbol{x})\cdot\delta Q_j(t',\boldsymbol{x}')\rangle = 2k\lambda\theta^2\delta_{ij}\delta(\boldsymbol{x}-\boldsymbol{x}')\delta(t-t'). \quad (7)$$

In Eqs. (1)–(3), we express $\rho = \rho_0 + \delta\rho$, $\boldsymbol{v} = \delta\boldsymbol{v}$, and $\theta = \theta_0 + \delta\theta$, where ρ_0, $\boldsymbol{v}_0 = 0$, and θ_0 are quantities under the static equilibrium state. Substituting $\rho = \rho_0 + \delta\rho$, $\boldsymbol{v} = \delta\boldsymbol{v}$ and $\theta = \theta_0 + \delta\theta$ in Eqs. (1)–(3) and neglecting nonlinear terms, we obtain

$$\frac{\partial\delta\rho}{\partial t} = -\rho_0(\nabla\cdot\delta\boldsymbol{v}), \quad (8)$$

$$\begin{aligned}\rho_0\frac{\partial(\delta\boldsymbol{v})}{\partial t} &= -\frac{1}{G_0}\nabla(\delta p) + \eta'\nabla^2\delta\boldsymbol{v} \\ &\quad + \left(\zeta' + \frac{1}{3}\eta'\right)\nabla(\nabla\cdot\delta\boldsymbol{v}) + \nabla\cdot\delta\Pi', \end{aligned}\quad (9)$$

$$\rho_0 c_v\frac{\partial\delta\theta}{\partial t} = \lambda\nabla^2\delta\theta - p_0(\nabla\cdot\delta\boldsymbol{v}) - \nabla\cdot\delta\boldsymbol{Q}, \quad (10)$$

where $p_0 = \rho_0\theta k/m$, $G_0 = G(\theta_0)$, $\eta' = \eta/G_0$, $\zeta' = \zeta/G_0$, and $\delta\Pi' = \delta\Pi/G_0$. Additionally, $\delta p = p_0(\delta\rho/\rho_0 + \delta\theta/\theta_0)$. To set variables $\delta\rho$, $\psi = \nabla\cdot\delta\boldsymbol{v}$ and $\delta\theta$ as independent variables, we take a divergence of both sides of Eq. (9) and obtain the following equation:

$$\begin{aligned}\rho_0\frac{\delta\psi}{\partial t} &= -p_0'\nabla^2\left(\frac{\delta\theta}{\theta_0} + \frac{\delta\rho}{\rho_0}\right) + \left(\zeta' + \frac{4}{3}\eta'\right)\nabla^2(\delta\psi) \\ &\quad + \nabla\cdot(\nabla\cdot\delta\Pi'), \end{aligned}\quad (11)$$

where $p_0' = p_0/G_0$.

Next, we transform $\delta\rho(t,\boldsymbol{x})$, $\delta\psi(t,\boldsymbol{x})$, $\delta\theta(t,\boldsymbol{x})$, $\delta\Pi(t,\boldsymbol{x})$, and $\delta\boldsymbol{Q}(t,\boldsymbol{x})$ into $\delta\rho(\omega,\boldsymbol{q})$, $\delta\psi(\omega,\boldsymbol{q})$, $\delta\theta(\omega,\boldsymbol{q})$, $\delta\Pi(\omega,\boldsymbol{q})$, and $\delta\boldsymbol{Q}(\omega,\boldsymbol{q})$ using Fourier transform, where ω is the frequency and $\boldsymbol{q}$ is the wave vector. For example, $\delta\rho(\omega,\boldsymbol{q}) = \int_0^\infty\int_{R^3}\exp\{2\pi i(\omega t - \boldsymbol{q}\cdot\boldsymbol{x})\}\delta\rho(t,\boldsymbol{x})d\boldsymbol{x}dt$, where R^3 indicates three-dimensional physical space. Finally, Eqs. (8), (11), and (10) are rewritten in $(\omega,\boldsymbol{q})$ space as

$$G^{-1}(\omega,q)\begin{pmatrix}\delta\rho(\omega,\boldsymbol{q})\\ \delta\psi(\omega,\boldsymbol{q})\\ \delta\theta(\omega,\boldsymbol{q})\end{pmatrix} = \boldsymbol{F}(\omega,\boldsymbol{q}), \quad (12)$$

where the matrix G^{-1} is the inverse linear response function, and $\boldsymbol{F} = (F_1, F_2, F_3)$ expresses the random force vector. G^{-1} and $\boldsymbol{F}$ are obtained from Eqs. (8), (11), and (10) as

$$G^{-1}(\omega,q) = \begin{pmatrix} i\omega & \rho_0 & 0 \\ -\frac{c_s^2q^2}{\gamma\rho_0} & (i\omega + D_Vq^2) & \frac{c_s^2q^2}{\gamma\theta_0} \\ 0 & (\gamma-1)\theta_0 & (i\omega + \gamma a_Tq^2)\end{pmatrix}, \quad (13)$$

$$\boldsymbol{F}(\omega,\boldsymbol{q}) = \frac{-1}{\rho_0}\begin{pmatrix}0\\ q_iq_j\delta\Pi_{ij}'(\omega,\boldsymbol{q})\\ iq_i\delta Q_i(\omega,\boldsymbol{q})/c_v\end{pmatrix}, \quad (14)$$

where $c_s = \sqrt{\gamma Gk\theta_0/m}$ is the speed of sound of thermally relativistic fluids, $D_V = (\zeta' + 4/3\eta')/\rho_0$ is the modified longitudinal kinematic viscosity of thermally relativistic fluids, and $a_T = \lambda/\rho_0c_p$ is the thermal diffusivity, in which c_p is the specific heat at the constant pressure, and $\gamma = c_p/c_v$.

Multiplying the matrix G in both sides of Eq. (12), we obtain

$$\begin{pmatrix} \delta\rho(\omega,\boldsymbol{q}) \\ \delta\psi(\omega,\boldsymbol{q}) \\ \delta\theta(\omega,\boldsymbol{q}) \end{pmatrix} = \begin{bmatrix} -\rho_0(i\omega+\gamma a_T q^2) \\ i\omega(i\omega+\gamma a_T q^2) \\ -i\omega(\gamma-1)\theta_0 \end{bmatrix} \frac{F_2(\omega,\boldsymbol{q})}{\det[G^{-1}(\omega,\boldsymbol{q})]} + \begin{bmatrix} -\rho_0\frac{c_s^2q^2}{\gamma\theta_0} \\ i\omega\rho_0\frac{c_s^2q^2}{\gamma} \\ \frac{c_s^2q^2}{\gamma}-\omega^2+i\omega D_V q^2 \end{bmatrix} \frac{F_3(\omega,\boldsymbol{q})}{\det[G^{-1}(\omega,\boldsymbol{q})]}, \tag{15}$$

where $\det[G^{-1}(\omega,\boldsymbol{q})]$ can be calculated under two constraints, namely, $c_s q \gg a_T q^2$ and $c_s q \gg D_V q^2$, as

$$\det[G^{-1}(\omega,q)] = (i\omega + a_T q^2)[i(\omega - c_s q) + \hat{\Gamma}_s q^2] \times [i(\omega + c_s q) + \hat{\Gamma}_s q^2], \tag{16}$$

where $\hat{\Gamma}_s = \frac{1}{2}[D_V + (\gamma - 1)a_T]$ is the modified sound attenuation coefficient of thermally relativistic fluids.

Finally, the autocorrelation between random force in $(\omega,\boldsymbol{q})$ space, namely, $\langle F_\alpha^*(\omega,\boldsymbol{q})F_\beta(\omega',\boldsymbol{q}')\rangle$, is obtained using the double Fourier transform of Eqs. (6) and (7) and the relation $\Pi' = \Pi/G_0$ as

$$\langle F_\alpha^*(\omega,\boldsymbol{q})F_\beta(\omega',\boldsymbol{q}')\rangle = C_{\alpha\beta}(2\pi)^4\delta(\omega-\omega')\delta(\boldsymbol{q}-\boldsymbol{q}'), \tag{17}$$

where $C_{\alpha\beta}$ $(\alpha,\beta = 1,2,3)$ is the element of the matrix C, which is formulated as

$$C(q) = \frac{2k\theta_0}{\rho_0}\begin{pmatrix} 0 & 0 & 0 \\ 0 & D_V q^4 & 0 \\ 0 & 0 & \frac{\theta_0\lambda}{\rho_0 c_v^2}q^2 \end{pmatrix}. \tag{18}$$

The autocorrelation of density fluctuations, namely, $\langle\delta\rho^*(\omega,\boldsymbol{q})\delta\rho(\omega,\boldsymbol{q})\rangle = \rho_0 m_0 S(\omega,q)(2\pi^4)\delta(\omega-\omega')\delta(\boldsymbol{q}-\boldsymbol{q}')$, is obtained from Eqs. (15)–(18), where $S(\omega,q)$ is the dynamic structure factor of thermally relativistic fluids. $S(\omega,q)$ is calculated from Eqs. (15)–(18) as

$$S(\omega,q) = \frac{2\frac{k}{m}\theta_0 q^2[(\gamma-1)c_s^2 a_T q^4 + (\omega^2+\gamma^2a_T^2q^4)D_V q^2]}{(\omega^2+a_T^2q^4)[(\omega-c_sq)^2+\hat{\Gamma}_s^2q^4][(\omega+c_sq)^2+\hat{\Gamma}_s^2q^4]}. \tag{19}$$

The form of $S(\omega,q)$ in Eq. (19) coincides with that of the nonrelativistic fluids, namely, $S_{\rm nr}(\omega,q)$ [13], when $G = 1$. $S_{\rm nr}(\omega,q)$ of the nonrelativistic fluids was reduced to $S_{\rm nr} = \frac{\gamma-1}{\gamma}\frac{2a_Tq^2}{\omega^2+a_T^2q^4} + \frac{1}{\gamma}[\frac{\hat{\Gamma}_sq^2}{(\omega+c_sq)^2+\hat{\Gamma}_s^2q^4} + \frac{\hat{\Gamma}_sq^2}{(\omega-c_sq)^2+\hat{\Gamma}_s^2q^4}]$ using two constraints, namely, $c_sq \gg a_Tq^2$ and $c_sq \gg D_Vq^2$, when the fluid is gas. Similarly, we reduce $S(\omega,q)$ in Eq. (19) using these two constraints as

$$S = \frac{\gamma-1}{\gamma}\frac{2a_Tq^2}{\omega^2+a_T^2q^4} + \frac{1}{\gamma}\left[\frac{\hat{\Gamma}_sq^2}{(\omega+c_sq)^2+\hat{\Gamma}_s^2q^4} + \frac{\hat{\Gamma}_sq^2}{(\omega-c_sq)^2+\hat{\Gamma}_s^2q^4}\right]. \tag{20}$$

From Eq. (20), the double inverse Fourier transform of $\langle\rho^*(\omega,\boldsymbol{q})\cdot\rho(\omega',\boldsymbol{q}')\rangle$ to $\langle\rho^*(t,\boldsymbol{q})\cdot\rho(t',\boldsymbol{q}')\rangle$ yields

$$\langle\rho^*(t,\boldsymbol{q})\cdot\rho(t',\boldsymbol{q}')\rangle = \rho m_0 S(q,|t-t'|)(2\pi)^3\delta(\boldsymbol{q}-\boldsymbol{q}'), \tag{21}$$

$$S(q,\tau) = \frac{\gamma-1}{\gamma}\exp(-a_Tq^2\tau) + \frac{1}{\gamma}\cos(c_sq\tau)\exp(-\hat{\Gamma}_sq^2\tau). \tag{22}$$

In this paper, we apply another form of $S(q,\tau)$, which was originally calculated for the nonrelativistic fluids by Boon and Yip [14], to the thermally relativistic fluids by reducing $S(\omega,q)$ in Eq. (19) as follows:

$$S(q,\tau) = \frac{\gamma-1}{\gamma}\exp(-a_Tq^2\tau) + \frac{1}{\gamma}\exp(-\hat{\Gamma}_sq^2\tau)\cos(c_sq\tau) + \frac{3\hat{\Gamma}_s - D_V}{\gamma^2 c_s}q\exp(-\hat{\Gamma}_sq^2\tau)\sin(c_sq\tau). \tag{23}$$

III. NUMERICAL ANALYSIS OF AUTOCORRELATION OF DENSITY FLUCTUATIONS FOR THERMALLY RELATIVISTIC FLUIDS

To investigate the autocorrelation of density fluctuations for thermally relativistic fluids, we solve the stochastic relativistic Boltzmann equation using the DSMC method. In previous studies, Garcia and his coworkers [15] calculated the autocorrelation of density fluctuations for the nonrelativistic gas and compared $\langle\rho^*(t,\boldsymbol{q})\cdot\rho(t',\boldsymbol{q}')\rangle$, which is obtained using the DSMC method, with $\langle\rho^*(t,\boldsymbol{q})\cdot\rho(t',\boldsymbol{q}')\rangle$, which is theoretically obtained by setting $\chi\to\infty$ in Eqs. (21) and (23). In this paper, we compare $\langle\rho^*(t,\boldsymbol{q})\cdot\rho(t',\boldsymbol{q}')\rangle$, which is calculated using the DSMC method, with $\langle\rho^*(t,\boldsymbol{q})\cdot\rho(t',\boldsymbol{q}')\rangle$, which is theoretically obtained by Eqs. (21) and (23). The algorithm to solve the stochastic relativistic Boltzmann equation using the DSMC method is described in our previous papers [6].

As the numerical condition, the system with the length l_∞ is set along the x axis, namely, $0 \le x \le l_\infty$, 128 cells, which have the common volume $dV = (l_\infty/128)^3$, are equally spaced along the x axis. $\mathrm{Kn} = 1/(\sigma_T n_\infty l_\infty) = 0.05$ (Kn: Knudsen number) corresponds to the transition regime between the continuum and rarefied regimes, where $\sigma_T = \pi d^2$ (d: diameter of a hard spherical particle) is the total collisional cross section, $n_\infty = N_c/dV$ is the number density. In our numerical analysis, $N_c = 100$ particles are set in a unit cell. The density is calculated using Eckart's decomposition [9]. Additionally, physical quantities, such as the density, spatial coordinate, and time, are normalized as $\tilde{\rho} = \rho/\rho_\infty$, $\tilde{x} = x/l_\infty$, $\tilde{t} = t/t_\infty$, in which $t_\infty = l_\infty/c$. The time step $\Delta\tilde{t}$ is set to $\Delta\tilde{t} = 0.005\pi$ Kn, and $N = 7.2 \times 10^6$ samples are used to calculate $\langle\tilde{\rho}^*(\tilde{t},\tilde{q}) \cdot \tilde{\rho}(\tilde{t}+\tilde{\tau},\tilde{q})\rangle$, in which $\tilde{q} = ql_\infty$. In the DSMC method, $\langle\tilde{\rho}^*(\tilde{t},2\pi) \cdot \tilde{\rho}(\tilde{t}+\tilde{\tau},2\pi)\rangle$ is calculated using the relation $\tilde{q} = 2\pi n$ $(n = 1, 2, 3, \ldots)$ as [15]

$$\langle\tilde{\rho}^*(\tilde{t},2\pi n)\cdot\tilde{\rho}(\tilde{t}+\tilde{\tau},2\pi n)\rangle = \frac{1}{N}\sum_{\text{samples}}^{N} R(\tilde{t})R(\tilde{t}+\tilde{\tau}),$$
$$R(\tilde{t}) = \frac{1}{M_c}\sum_{i=1}^{M_c}\tilde{\rho}_i\sin(2\pi n\tilde{x}_i), \tag{24}$$

where $\tilde{\rho}_i$ is the normalized density in the ith cell, $M_c = 128$ is the number of cells, x_i is the coordinate of the center of the ith cell. In the DSMC method [15], the theoretical value of $\langle\delta\tilde{\rho}^*(t,\boldsymbol{q}) \cdot \delta\tilde{\rho}(t,\boldsymbol{q})\rangle$ is obtained as $1/(2M_cN_c) = 3.91 \times 10^{-5}$.

A. Numerical results of autocorrelation of density fluctuations in the lowest wave number for thermally relativistic fluids

Here, we restrict ourselves to the autocorrelation of density fluctuations in the lowest wave number, namely, $n = 1$ in Eq. (24). As a result, $\tilde{q} = 2\pi$ is considered.

Figure 1 shows $\langle\tilde{\rho}^*(\tilde{t},2\pi) \cdot \tilde{\rho}(\tilde{t}+\tilde{\tau},2\pi)\rangle$ versus τ for $\chi = 2.9 \times 10^{-3}$, 0.5, 4.79 and 100. As shown in Fig. 1, the frequency of $\langle\tilde{\rho}^*(\tilde{t},2\pi) \cdot \tilde{\rho}(\tilde{t}+\tilde{\tau},2\pi)\rangle$ decreases, as χ increases. Meanwhile, $\langle\tilde{\rho}^*(\tilde{t},2\pi) \cdot \tilde{\rho}(\tilde{t}+\tilde{\tau},2\pi)\rangle$ for $\chi = 2.9 \times 10^{-3}$ is similar to $\langle\tilde{\rho}^*(\tilde{t},2\pi) \cdot \tilde{\rho}(\tilde{t}+\tilde{\tau},2\pi)\rangle$ for $\chi = 0.5$, whereas the damp of $\langle\tilde{\rho}^*(\tilde{t},2\pi) \cdot \tilde{\rho}(\tilde{t}+\tilde{\tau},2\pi)\rangle$ in a period for $\chi = 0.5$ is larger than that for $\chi = 2.9 \times 10^{-3}$. As shown in the upper-right frame of Fig. 1, $\langle\delta\tilde{\rho}^*(t,\boldsymbol{q}) \cdot \delta\tilde{\rho}(t,\boldsymbol{q})\rangle = 3.93 \times 10^{-5}$ for $\chi = 2.9 \times 10^{-3}$, 4.02×10^{-5} for $\chi = 0.5$, and 3.9×10^{-5} and 3.92×10^{-5} for $\chi = 100$ are similar to the theoretical value 3.91×10^{-5}.

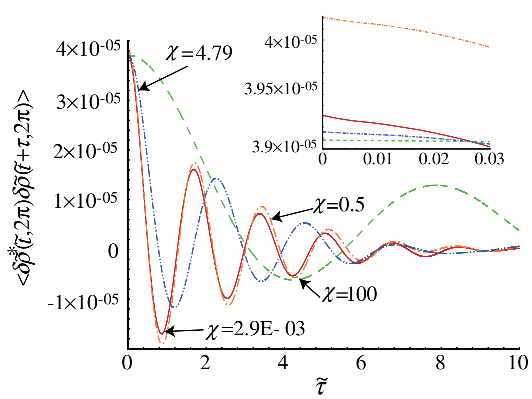

FIG. 1 (color online). $\langle\tilde{\rho}^*(\tilde{t},2\pi) \cdot \tilde{\rho}(\tilde{t}+\tilde{\tau},2\pi)\rangle$ versus $\tilde{\tau}$.

Figure 2 shows $\langle\tilde{\rho}^*(\tilde{t},2\pi) \cdot \tilde{\rho}(\tilde{t}+\tilde{\tau},2\pi)\rangle/\langle\tilde{\rho}^*(\tilde{t},2\pi) \cdot \tilde{\rho}(\tilde{t},2\pi)\rangle(= S(\tilde{\tau},2\pi))$ versus τ for $\chi = 2.9 \times 10^{-3}$ (top left), $\chi = 0.5$ (top middle), $\chi = 2.11$ (top right), $\chi = 4.79$ (bottom left), $\chi = 24.3$ (bottom middle) and $\chi = 100$ (bottom right), which are obtained using the DSMC method and theoretical result in Eq. (23). As shown in Fig. 2, $\langle\tilde{\rho}^*(\tilde{t},2\pi) \cdot \tilde{\rho}(\tilde{t}+\tilde{\tau},2\pi)\rangle/\langle\tilde{\rho}^*(\tilde{t},2\pi) \cdot \tilde{\rho}(\tilde{t},2\pi)\rangle$ obtained using the DSMC method is similar to $\langle\tilde{\rho}^*(\tilde{t},2\pi) \cdot \tilde{\rho}(\tilde{t}+\tilde{\tau},2\pi)\rangle/\langle\tilde{\rho}^*(\tilde{t},2\pi) \cdot \tilde{\rho}(\tilde{t},2\pi)\rangle$ obtained by Eq. (23) in a half period, namely, $0 \le 2c_s\pi\tau \le \pi$, in cases of $\chi = 4.79$ and 24.3, whereas $\langle\tilde{\rho}^*(\tilde{t},2\pi) \cdot \tilde{\rho}(\tilde{t}+\tilde{\tau},2\pi)\rangle/\langle\tilde{\rho}^*(\tilde{t},2\pi) \cdot \tilde{\rho}(\tilde{t},2\pi)\rangle$ obtained using the DSMC method is slightly different from $\langle\tilde{\rho}^*(\tilde{t},2\pi) \cdot \tilde{\rho}(\tilde{t}+\tilde{\tau},2\pi)\rangle/\langle\tilde{\rho}^*(\tilde{t},2\pi) \cdot \tilde{\rho}(\tilde{t},2\pi)\rangle$ obtained by Eq. (23) at a half period in cases of $\chi = 2.9 \times 10^{-3}$, 0.5, 2.11, and 100. Table I shows χ versus $a_T/(cl_\infty)$, $D_V/(cl_\infty)$, c_s/c, $\hat{\Gamma}_s/(cl_\infty)$, and γ. The similarity between $\langle\tilde{\rho}^*(\tilde{t},2\pi) \cdot \tilde{\rho}(\tilde{t}+\tilde{\tau},2\pi)\rangle/\langle\tilde{\rho}^*(\tilde{t},2\pi) \cdot \tilde{\rho}(\tilde{t},2\pi)\rangle$ for $\chi = 2.9 \times 10^{-3}$ and that for $\chi = 0.5$ is described by similarities between a_T, D_V, c_s, $\hat{\Gamma}_s$, and γ for $\chi = 2.9 \times 10^{-3}$ and those for $\chi = 0.5$, as shown in Table I. a_T, $\hat{\Gamma}_s$, and D_V, which are related to the damping rate of $S(\tau,q)$, decrease as χ increases, and c_s, which is related to the frequency of $S(\tau,q)$ decreases as χ increases, and $1/\gamma$, which is related to the amplitude of $S(\tau,q)$, decreases as χ increases, as shown in Table I.

As shown in Fig. 2, $\langle\tilde{\rho}^*(\tilde{t},2\pi)\cdot\tilde{\rho}(\tilde{t}+\tilde{\tau},2\pi)\rangle/\langle\tilde{\rho}^*(\tilde{t},2\pi)\cdot\tilde{\rho}(\tilde{t},2\pi)\rangle$ obtained using the DSMC method is markedly different from that obtained by Eq. (23) at a period, namely, $2\pi c_s\tau = 2\pi$. Such a marked difference at a period is also obtained for the nonrelativistic fluids by Bell *et al.* [15]. Additionally, the frequency of the $\langle\tilde{\rho}^*(\tilde{t},2\pi)\cdot\tilde{\rho}(\tilde{t}+\tilde{\tau},2\pi)\rangle/\langle\tilde{\rho}^*(\tilde{t},2\pi) \cdot \tilde{\rho}(\tilde{t},2\pi)\rangle$ obtained using the DSMC method increases from $2\pi c_s$ at $2\pi \le 2\pi c_s\tau$ for all the cases of χ, as shown in Fig. 2. We, however, can conclude that Eqs. (21) and (23) accurately reproduce the autocorrelation of density fluctuations for thermally relativistic fluids in the lowest wave number, which are composed of hard spherical particles, whereas the effect of acausality in Eqs. (2) and (3) or effects of eliminations of nonlinear terms in Eqs. (A2) and (A3) and the term $-Dq^\alpha/c^2$ in Eq. (A4) on the theoretical result in Eq. (23) are set to our future study. Finally, we confirmed that $\langle\tilde{\rho}^*(\tilde{t},2\pi)\cdot\tilde{\rho}(\tilde{t}+\tilde{\tau},2\pi)\rangle/\langle\tilde{\rho}^*(\tilde{t},2\pi)\cdot\tilde{\rho}(\tilde{t},2\pi)\rangle$ obtained by Eq. (22) is quite similar to that obtained by Eq. (23).

B. Numerical results of autocorrelation of density fluctuations in high wave number under thermally ultrarelativistic limit

We confirmed that Eqs. (21) and (23) reproduce the autocorrelation of density fluctuations in the lowest wave number for thermally relativistic fluids, which is obtained using the DSMC method, with good accuracy. Here, we investigate the autocorrelation of density fluctuations in the high wave number, namely, $1 < n$ in Eq. (24), under the thermally ultrarelativistic limit, namely, $\chi \ll 1$. The

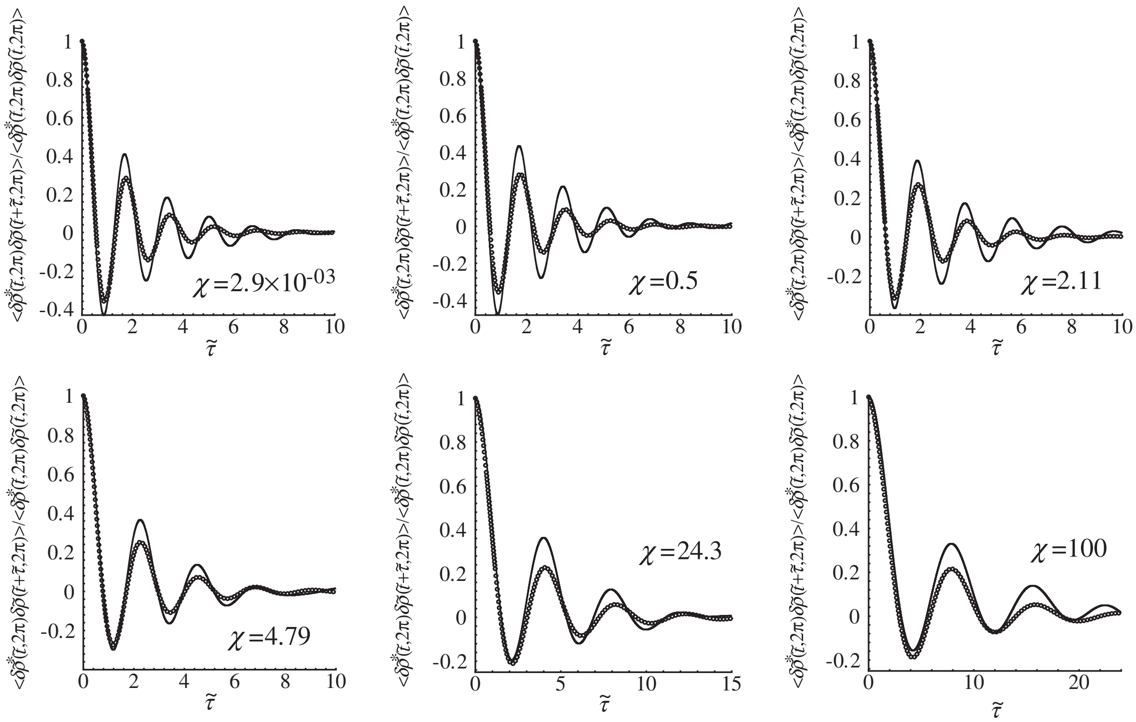

FIG. 2. $\langle \tilde{\rho}^*(\tilde{t}, 2\pi) \cdot \tilde{\rho}(\tilde{t} + \tilde{\tau}, 2\pi)\rangle / \langle \tilde{\rho}^*(\tilde{t}, 2\pi) \cdot \tilde{\rho}(\tilde{t}, 2\pi)\rangle$ versus $\tilde{\tau}$ for $\chi = 2.9 \times 10^{-3}$ (top left), $\chi = 0.5$ (top middle), $\chi = 2.11$ (top right), $\chi = 4.79$ (bottom left), $\chi = 24.3$ (bottom middle) and $\chi = 100$ (bottom right). Lines express DSMC results and symbols express theoretical results in Eq. (23).

autocorrelation of density fluctuations in the lowest wave number under the thermally ultrarelativistic limit has been already discussed in the case of $\chi = 2.9 \times 10^{-3}$ in Figs. 1 and 2. The comparison of the theoretical result of the autocorrelation of density fluctuations in the high wave number [$1 < n$ in Eq. (24)] under the thermally ultrarelativistic limit with the numerical result obtained using the DSMC method is significant for understanding of the limit of the accuracy of the theoretical result in Eq. (23) under the transition regime between rarefied and continuum regimes, namely, $\mathrm{Kn} = 0.05$. We can easily predict that the autocorrelation of density fluctuations in the higher wave number must be described using the larger Kn, because density fluctuations in the higher wave number describe density fluctuations in the smaller scale. In other words, fluctuations of the distribution function in the smaller scale must be described using fluctuations of nonequilibrium moments beyond 14 moments. Therefore, Garcia and his coworkers [15] did not compare the theoretical result of density fluctuations for the nonrelativistic fluids in the high wave number ($1 < n$) with that obtained using the DSMC method for the stochastic nonrelativistic Boltzmann equation [15] under the transition regime. For numerical comparisons, we calculate the autocorrelation of density fluctuations under the thermally relativistic limit, namely, $\chi = 2.9 \times 10^{-3}$ in Eqs. (21) and (23) using transport coefficients, which were calculated by Denicol *et al.* [16], whereas we used transport coefficients, which were calculated by Cercignani and Kremer on the basis of Israel-Stewart theory [9], in the above discussions. Denicol *et al.* [16] formulated transport coefficient by expanding the distribution function with all moments in the relativistic Boltzmann equation. Consequently, transport coefficients, which are calculated by Denicol *et al.*, are different

TABLE I. $a_T/(cl_\infty)$, $D_V/(cl_\infty)$, c_s/c, $\hat{\Gamma}_s/(cl_\infty)$ and γ versus χ.

χ	$a_T/(cl_\infty)$	$D_V/(cl_\infty)$	c_s/c	$\hat{\Gamma}_s/(cl_\infty)$	γ
2.9×10^{-3}	3.33×10^{-2}	0.02	0.577	1.55×10^{-2}	1.33
0.5	3.28×10^{-2}	1.96×10^{-2}	0.572	1.54×10^{-2}	1.34
2.11	2.9×10^{-2}	1.72×10^{-2}	0.521	1.45×10^{-2}	1.41
4.79	2.41×10^{-2}	1.4×10^{-2}	0.441	1.28×10^{-2}	1.48
24.3	1.31×10^{-2}	7.21×10^{-3}	0.245	7.61×10^{-3}	1.65
100	6.81×10^{-3}	3.81×10^{-3}	0.127	4.11×10^{-3}	1.65

TABLE II. $a_T/(cl_\infty)$, $D_V/(cl_\infty)$ and $\hat{\Gamma}_s/(cl_\infty)$ obtained using η and κ (Israel-Stewart theory [9]), η_{14} and κ_{14} (14-moments approximation by Denicol *et al.* [16]), and η_{41} and κ_{41} (41-moments approximation by Denicol *et al.* [16]) in the case of $\chi = 2.9 \times 10^{-3}$.

Model	$a_T/(cl_\infty)$	$D_V/(cl_\infty)$	$\hat{\Gamma}_s/(cl_\infty)$
Israel-Stewart theory	3.33×10^{-2}	0.02	1.55×10^{-2}
14-moments approximation by Denicol *et al.*	5.0×10^{-2}	2.22×10^{-2}	1.94×10^{-2}
41-moments approximation by Denicol *et al.*	4.26×10^{-2}	2.11×10^{-2}	1.77×10^{-2}

from transport coefficients, which were calculated by Cercignani and Kremer on the basis of Israel-Stewart theory. Greif *et al.* [17] calculated the thermal conductivity of massless hard spherical particles from the heat flow, which is obtained by solving the relativistic Boltzmann equation and compared that with thermal conductivities, which are obtained using Israel-Stewart theory, N-moments approximation by Denicol *et al.*, and Chapman-Enskog method by Groot *et al.* [18].

Here, we use the viscosity coefficient and thermal conductivity, which were calculated using 14-moments approximation or 41-moments approximation under the thermally ultra-relativistic limit ($\chi \to 0$) by Denicol *et al.* [16], whereas the bulk viscosity, which was calculated by Cercignani and Kremer [9], is used, because the bulk viscosity approximates to zero under the thermally ultra-relativistic limit ($\chi = 2.9 \times 10^{-3}$). Transport coefficients under the thermally ultrarelativistic limit obtained using 41-moments approximation by Denicol *et al.* [16] are quite similar to those obtained by Groot *et al.* on the basis of Chapman-Enskog method [18]. η_{14} and η_{41}, which is the viscosity coefficient obtained using 14-moments

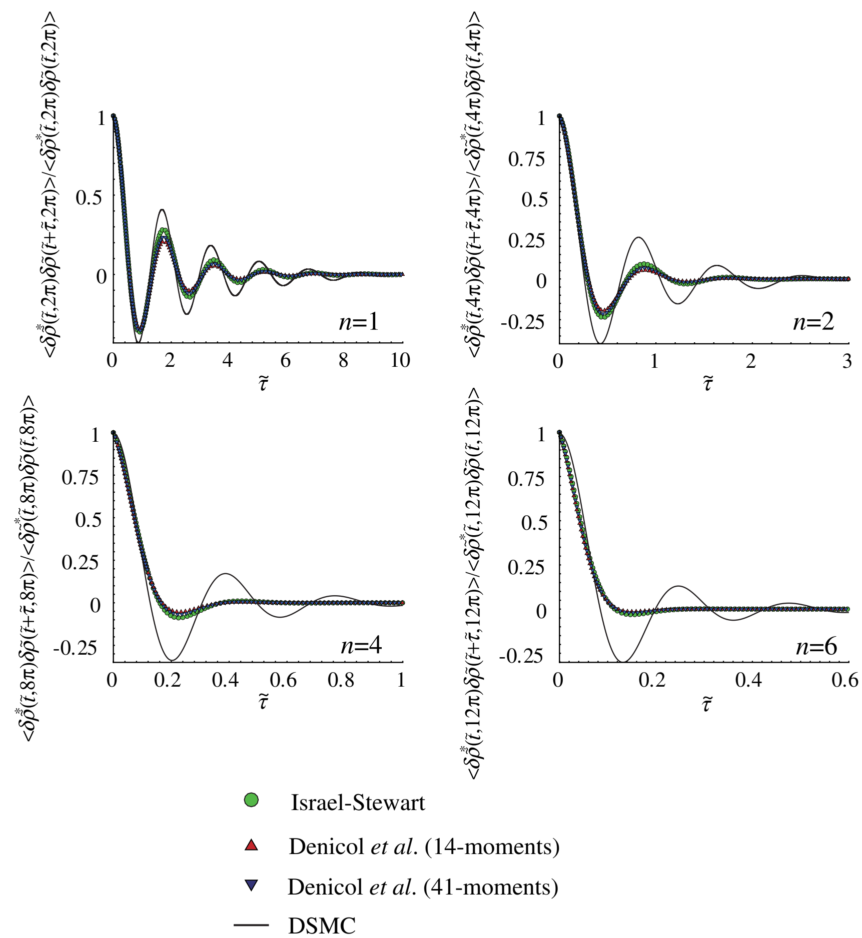

FIG. 3 (color online). $\langle\tilde{\rho}^*(\tilde{t}, 2\pi n) \cdot \tilde{\rho}(\tilde{t} + \tilde{\tau}, 2\pi n)\rangle / \langle\tilde{\rho}^*(\tilde{t}, 2\pi n) \cdot \tilde{\rho}(\tilde{t}, 2\pi n)\rangle$ versus $\tilde{\tau}$, which are obtained using Israel Stewart theory (circular symbols), 14-moments approximation by Denicol *et al.* (delta symbols), 41-moments approximation by Denicol *et al.* (gradient symbols), and DSMC method (lines) in cases of $n = 1$ (top left), 2 (top right), 4 (bottom left) and 6 (bottom right) in Eq. (24), when $\chi = 2.9 \times 10^{-3}$.

approximation or 41-moments approximation by Denicol *et al.* [16], respectively, are related to the viscosity coefficient obtained using Israel-Stewart theory (η) with $\eta_{14} = 10/9\eta$ and $\eta_{41} = 1.0558\eta$ under the thermally ultrarelativistic limit ($\chi \to 0$), whereas λ_{14} and λ_{41}, which is the thermal conductivity obtained using 14-moments approximation or 41-moments approximation by Denicol *et al.*, respectively, are related to the thermal conductivity obtained using Israel-Stewart theory (λ) with $\lambda_{14} = 3/2\lambda$ and $\lambda_{41} = 1.2768\lambda$ under the thermally ultrarelativistic limit ($\chi \to 0$). We apply these relations among transport coefficients under $\chi \to \epsilon \ll 2.9 \times 10^{-3}$ to those under $\chi = 2.9 \times 10^{-3}$.

Table II shows a_T, $\hat{\Gamma}_s$, and D_V, which are obtained using η_{14} and κ_{14} or η_{41} and κ_{41} together with a_T, $\hat{\Gamma}_s$, and D_V obtained using η and κ in the case of $\chi = 2.9 \times 10^{-3}$, in which a_T, $\hat{\Gamma}_s$, and D_V are related to the damping rate of $S(\tau, q)$, as shown in Eq. (23). We can easily confirm that a_T, $\hat{\Gamma}_s$, and D_V in the case of $\chi = 2.9 \times 10^{-3}$ are almost equal to those in the case of $\chi \to \epsilon \ll 2.9 \times 10^{-3}$. As a result, the above application of the relation among transport coefficients under $\chi \to \epsilon \ll 2.9 \times 10^{-3}$ to that under the relation under $\chi = 2.9 \times 10^{-3}$ is correct. Table II indicates that the damping rate of $S(\tau, q)$ obtained using η_{14} and κ_{14} is the highest, whereas the damping rate of $S(\tau, q)$ obtained using η and κ is the lowest.

Figure 3 shows $\langle \tilde{\rho}^*(\tilde{t}, 2\pi n) \cdot \tilde{\rho}(\tilde{t} + \tilde{\tau}, 2\pi n)\rangle / \langle \tilde{\rho}^*(\tilde{t}, 2\pi n) \cdot \tilde{\rho}(\tilde{t}, 2\pi n)\rangle$ in cases of $n = 1$ (top left), $n = 2$ (top right), $n = 4$ (bottom left) and $n = 6$ (bottom right), which are obtained using transport coefficients by Israel-Stewart theory (circular symbols), 14-moments approximation by Denicol *et al.* (delta symbols), and 41-moments approximation by Denicol *et al.* (gradient symbols). As predicted from Table II, the damping rate of $\langle \tilde{\rho}^*(\tilde{t}, 2\pi n) \cdot \tilde{\rho}(\tilde{t} + \tilde{\tau}, 2\pi n)\rangle / \langle \tilde{\rho}^*(\tilde{t}, 2\pi n) \cdot \tilde{\rho}(\tilde{t}, 2\pi n)\rangle$ obtained using 14-moments approximation by Denicol *et al.* is the highest in cases of $n = 1$, 2, 4, and 6, whereas the damping rate of $\langle \tilde{\rho}^*(\tilde{t}, 2\pi n) \cdot \tilde{\rho}(\tilde{t} + \tilde{\tau}, 2\pi n)\rangle / \langle \tilde{\rho}^*(\tilde{t}, 2\pi n) \cdot \tilde{\rho}(\tilde{t}, 2\pi n)\rangle$ obtained using Israel-Stewart theory is the lowest in cases of $n = 1$, 2, 4, and 6. Meanwhile, the damping rate of $\langle \tilde{\rho}^*(\tilde{t}, 2\pi n) \cdot \tilde{\rho}(\tilde{t} + \tilde{\tau}, 2\pi n)\rangle / \langle \tilde{\rho}^*(\tilde{t}, 2\pi n) \cdot \tilde{\rho}(\tilde{t}, 2\pi n)\rangle$ obtained using the DSMC method is lower than those obtained using transport coefficients by Israel-Stewart theory, 14-moments approximation by Denicol *et al.*, and 41-moments approximation by Denicol *et al.* in cases of $n = 1, 2, 4$ and 6. In particular, such difference between the damping rate obtained using the DSMC method and theoretical results in Eq. (23) increases, as n increases. Consequently, the theoretical result of the autocorrelation of density fluctuations under the thermally ultrarelativistic limit in Eq. (23) is insufficient to describe the autocorrelation of density fluctuations under the thermally ultrarelativistic limit, which is obtained using the stochastic relativistic Boltzmann equation, in the high wave number ($1 < n$). We, however, note that such an insufficiency of the theoretical result in Eq. (23) in the high wave number ($1 < n$) is presumably caused by rarefied effects, which cannot be expressed by the thermally relativistic NSF equation in Eqs. (8)–(10). In short, the fluctuation of the distribution function is not always described in the framework of 14 moments, when the scale of fluctuations is adequately small, in which the autocorrelation of density fluctuations is affected by fluctuations of nonequilibrium moments beyond 14 moments.

IV. DISCUSSION

Numerical results of the autocorrelation of density fluctuations obtained using the DSMC method indicate that the description of the thermal fluctuations in the framework of the relativistic NSF equation in Eqs. (8)–(10) is accurate enough to demonstrate the autocorrelation of density fluctuations for massive hard spherical particles under the static equilibrium state, when we restrict ourselves to the autocorrelation of density fluctuations in the lowest wave number. Meanwhile, effects of fluctuations of nonequilibrium moments beyond 14 moments are significant for the autocorrelation of density fluctuations in the high wave number owing to rarefied effects. Consequently, we consider that our theoretical formulation of the autocorrelation of density fluctuations for thermally relativistic fluids in Eqs. (21) and (23) is useful for understanding of the autocorrelation of density fluctuations for thermally relativistic fluids, when effects of fluctuations of nonequilibrium moments beyond 14 moments on the autocorrelation of density fluctuations for thermally relativistic fluids are ignorable even for the high wave number owing to Kn $\ll 1$. On the contrary, the DSMC calculation in the regime of Kn $\ll 1$ is difficult owing to the marked increase of the number of particles even with the most advanced supercomputer. Provided that we can calculate the autocorrelation of density fluctuations for thermally relativistic fluids under Kn $\ll 1$ using the DSMC method, we can conclude which transport coefficients among those obtained using Israel-Stewart theory, 14-moment approximation by Denicol *et al.* and 41-moment approximation by Denicol *et al.* reproduce the autocorrelation of density fluctuations for thermally relativistic fluids, which is obtained using the DSMC method, with the best accuracy.

Consequently, we expect that the dynamic structure factor $S(q, \tau)$ in Eqs. (22) and (23) can be extended by changing η, ζ and λ for hard spherical particles to η, ζ and λ, which are analytically determined or experimentally obtained for the QGP. Simultaneously, the binary collisional mechanics for hard spherical particles in the DSMC method must be changed to that for the QGP to compare the autocorrelation of density fluctuations for the QGP obtained using Eqs. (1)–(3) with the autocorrelation of density fluctuations for the QGP obtained using the DSMC method.

As a future study, we must investigate the autocorrelation of density fluctuations under $v \sim c$. In this paper, we can use Eqs. (2) and (3) under the assumption of $v \ll c$, as described in the Appendix. Meanwhile, nonlinear terms, which are eliminated in Eqs. (2) and (3), are significant to describe the relativistic NSF equation with thermal fluctuations. In particular, thermal fluctuations under the flow with $v \sim c$ are significant for understanding of the characteristics of thermal fluctuations inside the Mach cone of the QGP. Of course, the fluctuation-dissipation theorem, which is formulated under the equilibrium state, must be extended to the fluctuation-dissipation theorem under the strongly nonequilibrium state to describe thermal fluctuations inside the Mach cone [19].

In the above discussion on the autocorrelation of density fluctuations for thermally relativistic fluids, we restrict ourselves to flat spacetime. Meanwhile, we must consider the autocorrelation of density fluctuations for the thermal relativistic fluids in curved spacetime [20], when the thermally relativistic fluids in the early epoch of the universe are addressed. Such an autocorrelation of density fluctuations for thermally relativistic fluids in the early epoch of the universe will be investigated by solving the stochastic general relativistic Boltzmann equation, which is coupled to Einstein's equation [21]. Of course, the development of the robust numerical scheme, which solves Einstein's equation with the fluctuating energy-momentum tensor owing to thermal fluctuations, might be required.

V. CONCLUDING REMARKS

In this paper, we investigated the autocorrelation of density fluctuations for thermally relativistic fluids, which are composed of massive hard spherical particles under the transition regime, both theoretically and numerically. The autocorrelation of density fluctuations for thermally relativistic fluids obtained using the DSMC method indicates good agreements with the autocorrelation of density fluctuations for thermally relativistic fluids, which is theoretically obtained using the relativistic NSF equation, in the range of $2.9 \times 10^{-3} \leq \chi \leq 100$, when we restrict ourselves to the autocorrelation of density fluctuations in the lowest wave number. The difference between the autocorrelation of density fluctuations for thermally relativistic fluids obtained using the DSMC method and that obtained using the thermally relativistic NSF equation increases, as the wave number of the autocorrelation of density fluctuations increases under the thermally ultrarelativistic limit, whereas the choice of transport coefficients in accordance with the kinetic scheme does not make such a difference between the autocorrelation of density fluctuations for the thermally relativistic fluids obtained using the DSMC method and that obtained using the thermally relativistic NSF equation in the high wave number. Consequently, we consider that our theoretical formulation of the autocorrelation of density fluctuations for the thermally relativistic fluids is useful for understanding of the autocorrelation of density fluctuations for the QGP by applying transport coefficients of the QGP to our theoretical formulation of the autocorrelation of density fluctuations for the thermally relativistic fluids, when effects of fluctuations of nonequilibrium moments beyond 14 moments on the autocorrelation of density fluctuations for the thermally relativistic fluids are ignorable even for the high wave number owing to Kn $\ll 1$.

ACKNOWLEDGMENTS

The authors gratefully acknowledge Professor Tetsufumi Hirano (Sophia University, Tokyo, Japan) for discussions on the thermally fluctuating relativistic hydrodynamics of the QGP.

APPENDIX: DERIVATION OF RELATIVISTIC NAVIER-STOKES-FOURIER EQUATION IN EQ. (1)–(3)

Balance equations of the mass, momentum density, and energy density are written in Eckart's frame as [9]

$$Dn + n\nabla^\alpha U_\alpha = 0, \tag{A1}$$

$$\begin{aligned} \frac{nh_E}{c^2} DU^\alpha = {} & \nabla^\alpha(p + \Pi) - \nabla_\beta \pi^{\langle\alpha\beta\rangle} + \frac{1}{c^2}\Big(\pi^{\langle\alpha\beta\rangle} DU_\beta \\ & - \Pi DU^\alpha - Dq^\alpha - q^\alpha \nabla_\beta U^\beta - q^\beta \nabla_\beta U^\alpha \\ & - \frac{1}{c^2} U^\alpha q^\beta DU_\beta - U^\alpha \pi^{\langle\beta\gamma\rangle} \nabla_\beta U_\gamma \Big), \end{aligned} \tag{A2}$$

$$nDe = -(p + \Pi) + \pi^{\langle\alpha\beta\rangle}\nabla_\beta U_\alpha - \nabla_\alpha q^\alpha + \frac{2}{c^2} q^\alpha DU_\alpha, \tag{A3}$$

where $n = \rho/m$ is the number density, $U^\alpha = \gamma(v)(c, v_i)$ ($i = 1, 2, 3$, $\gamma(v) = 1/\sqrt{1 - v^2/c^2}$: Lorentz factor) is the four flow velocity, $D \equiv U^\alpha \nabla_\alpha$ is the convective time derivative, $\nabla^\alpha = \Delta^{\alpha\beta}\partial_\beta$, in which $\Delta^{\alpha\beta} = (\eta^{\alpha\beta} - U^\alpha U^\beta/c^2)\partial_\beta$, where $\eta^{\alpha\beta} = \mathrm{diag}(1, -1, -1, -1)$, is the projector, e is the energy density, and $h_E = mc^2 G$ is the enthalpy per particle.

In this paper, we investigate thermal fluctuations under static state in the laboratory frame. Then we assume that the product of nonlinear terms, which are expressed by products of U_α (or U^α) and $\pi^{\langle\alpha\beta\rangle}$, Π or q^α in Eqs. (A2) and (A3), are negligible owing to $\delta v_i \ll c$ ($i = 1, 2, 3$).

Consequently, linearized balance equations of the momentum density and energy density are written from Eqs. (A2) and (A3) by neglecting nonlinear terms as [9]

$$\frac{nh_E}{c^2}DU^\alpha = \nabla^\alpha(p+\Pi) - \nabla_\beta \pi^{\langle\alpha\beta\rangle} - \frac{1}{c^2}Dq^\alpha, \quad \text{(A4)}$$

$$nDe = -p\nabla_\beta U^\beta - \nabla_\beta q^\beta. \quad \text{(A5)}$$

In Eq. (A4), we assume that the term $-Dq^\alpha/c^2$ is negligible and rewrite Eq. (A4) as [22]

$$\frac{nh_E}{c^2}DU^\alpha = \nabla^\alpha(p+\Pi) - \nabla_\beta \pi^{\langle\alpha\beta\rangle}. \quad \text{(A6)}$$

From Eqs. (A1), (A5), and (A6), we readily obtain Eqs. (1)–(3) using relations $De = c_v D\theta$, $h_E = mc^2 G$, and $\gamma(v) = 1$.

[1] J. I. Kapusta, B. Müller, and M. Stephanov, Phys. Rev. C **85**, 054906 (2012).

[2] RHIC, http://www.bnl.gov/rhic/.

[3] LHC, http://home.web.cern.ch/.

[4] R. Yano and K. Suzuki, Phys. Rev. D **83**, 023517 (2011); **83**, 049901(E) (2011).

[5] M. E. Peskin and D. V. Schroeder, *An Introduction to Quantum Field Theory* (Addison-Wesley, Reading, MA, 1995).

[6] R. Yano and K. Suzuki, Phys. Rev. D **86**, 083522 (2012); R. Yano, J. Matsumoto, and K. Suzuki, Phys. Rev. D **83**, 123510 (2011).

[7] K. Yagi, T. Hatsuda, and Y. Miake, *Quark-Gluon Plasma* (Cambridge University Press, Cambridge, England, 2005).

[8] Z. Xu and C. Greiner, Phys. Rev. C **71**, 064901 (2005).

[9] C. Cercignani and G. M. Kremer, *The Relativistic Boltzmann Equation: Theory and Applications*, Progress in Math. Phys. (Springer-Verlag, Berlin, 2002), Vol. 22.

[10] Y. Minami and T. Kunihiro, Prog. Theor. Phys. **122**, 881 (2009).

[11] G. A. Bird, *Molecular Gas Dynamics and the Direct Simulation of Gas Flows* (Claredon, Oxford, England, 1994).

[12] E. Calzetta, Classical Quantum Gravity **15**, 653(E) (1998).

[13] J. M. Ortiz de Zarate and J. V. Sengers, *Hydrodynamic Fluctuations in Fluids and Fluid Mixtures* (Elsevier, New York, 2006).

[14] J. P. Boon and S. Yip, *Molecular Hydrodynamics* (Dover, New York, 1991).

[15] J. B. Bell, A. L. Garcia, and S. A. Williams, Phys. Rev. E **76**, 016708 (2007); A. Garcia, Phys. Rev. A **34**, 1454 (1986); M. M. Mansour, A. Garcia, G. Lie, and E. Clementi, Phys. Rev. Lett. **58**, 874 (1987).

[16] G. S. Denicol, H. Niemi, E. Molnar, and D. H. Rischke, Phys. Rev. D **85**, 114047 (2012).

[17] M. Greif, F. Reining, I. Bouras, G. S. Denicol, Z. Xu, and C. Greiner, Phys. Rev. E **87**, 033019 (2013).

[18] S. R. de Groot, W. A. van Leeuwen, and Ch. G. van Weert, *Relativistic Kinetic Theory* (Elsevier, New York, 1980).

[19] I. Bouras, E. Molnar, H. Niemi, Z. Xu, A. El, O. Fochler, F. Lauciello, C. Greiner, and D. H. Rischke, J. Phys. Conf. Ser. **230**, 012045 (2010).

[20] W. Zimdahl, Classical Quantum Gravity **6**, 1879 (1989).

[21] R. Yano, K. Suzuki, and H. Kuroda, Phys. Rev. D **80**, 123506 (2009).

[22] The term $-Dq^\alpha/c^2$ in Eq. (A4) might be significant, when $\theta \to \infty$, as shown in Eq. (7). Meanwhile, the contribution of the term Dq^α/c^2 in Eq. (A4) to the autocorrelation of the density is set for our future study.